Published in final edited form as:
Ophthalmology. 1999 March ; 106(3): 570–579.

Evaluation of Focal Defects of the Nerve Fiber Layer Using Optical Coherence Tomography

Liselotte Pieroth, MD[1], **Joel S. Schuman, MD**[1], **Ellen Hertzmark, MA**[1], **Michael R. Hee, MS**[2], **Jason R. Wilkins, BS**[1], **Jeffrey Coker, BS**[1], **Cynthia Mattox, MD**[1], **Tamar Pedut–Kloizman, MD**[1], **Carmen A. Puliafito, MD**[1], **James G. Fujimoto, PhD**[2], and **Eric Swanson**[3]

1 *New England Eye Center, Tufts University School of Medicine, Boston, Massachusetts*

2 *Massachusetts Institute of Technology, Cambridge, Massachusetts*

3 *MIT-Lincoln Laboratory, Lexington, Massachusetts*

Abstract

Objective— To analyze glaucomatous eyes with known focal defects of the nerve fiber layer (NFL), relating optical coherence tomography (OCT) findings to clinical examination, NFL and stereoscopic optic nerve head (ONH) photography, and Humphrey 24–2 visual fields.

Design— Cross-sectional prevalence study.

Participants— The authors followed 19 patients in the study group and 14 patients in the control group.

Intervention— Imaging with OCT was performed circumferentially around the ONH with a circle diameter of 3.4 mm using an internal fixation technique. One hundred OCT scan points taken within 2.5 seconds were analyzed.

Main Outcome Measures— Measurements of NFL thickness using OCT were performed.

Results— In most eyes with focal NFL defects, OCTs showed significant thinning of the NFL in areas closely corresponding to focal defects visible on clinical examination, to red-free photographs, and to defects on the Humphrey visual fields. Optical coherence tomography enabled the detection of focal defects in the NFL with a sensitivity of 65% and a specificity of 81%.

Conclusion— Analysis of NFL thickness in eyes with focal defects showed good structural and functional correlation with clinical parameters. Optical coherence tomography contributes to the identification of focal defects in the NFL that occur in early stages of glaucoma.

The early diagnosis of nerve fiber layer (NFL) changes is crucial for all patients with glaucoma. Once a visual field deficit is detectable, the disease has already caused irreversible visual loss.[1–4] Localized retinal NFL abnormalities and localized neuroretinal rim changes have been shown to precede visual field defects earlier than other signs detected during the conventional ophthalmologic examination.[5–7]

Glaucomatous changes in the NFL can be classified into those with focal nerve fiber damage, those with diffuse damage, and those with a combination of the two. A focal defect in the NFL corresponds with a wedge or bundle defect of the NFL, with its base reaching the horizontal fundus raphe and its tip touching the optic disc border in less than 60° of the disc circumference

Address correspondence to Joel S. Schuman, MD, New England Eye Center, New England Medical Center Hospitals, Tufts University School of Medicine, 750 Washington Street, Box 450, Boston, MA 02111.
Carmen A. Puliafito, MD, and James G. Fujimoto, PhD, are consultants to Humphrey Instruments, Inc., San Leandro, California.

Presented in part as a poster at the American Academy of Ophthalmology annual meeting, Chicago, Illinois, October, 1996.

and often a corresponding small deep visual field defect (indicated by corrected pattern standard deviation in the Humphrey visual field analyzer). In early glaucoma, bundle defects in the NFL may not affect the neuroretinal rim appearance because the damaged NFL is located in the deep retinal layers.[5,6,8–13] In cross-sectional studies, focal defects are found in approximately 20% of the glaucomatous eyes examined. Bundle defects can also occur in eyes with atrophy of the optic nerve because of other factors, such as optic disc drusen, toxoplasmic chorioretinal scars, ischemic retinopathy with cotton–wool spots of the retina, Leber's hereditary optic neuropathy, longstanding papilledema, and optic neuritis due to multiple sclerosis.[14] These defects are usually located in the inferotemporal and superotemporal fundus regions and are most often found in early, rather than advanced, glaucoma.[14,15] Bundle defects can also be associated with optic disc hemorrhages.[16,17] Unlike slitlike changes, localized NFL defects rarely occur in normal eyes.

Diffuse defects of the NFL are characterized by a generalized thinning of the NFL and often a loss of mean sensitivity in the visual field testing (indicated by baseline mean deviation in the automated visual fields). It is more difficult to detect diffuse defects of the NFL than to detect focal defects by conventional visual field techniques.

Most patients with glaucoma present with a localized defect of the NFL associated with diffuse thinning of the NFL; these findings may or may not be associated with localized or diffuse defects on visual field testing.

Conventional clinical tools (e.g., ophthalmoscopy) are subjective and show great variability with even experienced observers.[18] The interpretation of NFL photographs is influenced by the examiner's experience and the amount of melanin in the patient's pigment epithelium.[19] It also depends on the age of the patient. The shiny look of the retina prevents the focus of viewing on the NFL reflex in younger individuals.[10] Blue light improves the visualization of the retinal NFL, but in older patients with yellow discoloration of the lens, the clinical evaluation of the NFL is limited because of the filtering of blue light through the cataractous lens.[14] The neuroretinal rim and the optic disc show considerable interindividual variability.[20,21]

Optical coherence tomography (OCT) is a new optical device that permits a noncontact, high-resolution, and cross-sectional imaging of the anterior and posterior segment of the eye as well as quantitative assessment of different layers. Compared to current diagnostic techniques, OCT is not limited by ocular aperture, does not lack sensitivity nor reproducibility, and still achieves a high axial resolution of approximately 10 μm. In this study, we compared eyes with known focal defects of the NFL to eyes of glaucoma suspects and control patients using OCT and conventional clinical tools to evaluate glaucoma.

Patients and Methods

All patients examined between April 1994 and June 1996 at the New England Eye Center, Boston, Massachusetts, who met our criteria as study or control patients and who signed an informed consent approved by the Human Investigation Review Committee of New England Medical Center were included. All subjects underwent complete ophthalmologic examination including medical, ocular, and family history; visual acuity testing; Humphrey 24–2 visual field testing; undilated and dilated intraocular pressure (IOP) measurement; slit-lamp stereo biomicroscopy; indirect ophthalmoscopy; NFL and stereoscopic ONH photography; and OCT examination during each visit. All 24–2 Humphrey visual fields, NFL, and optic disc stereophotographs were reviewed separately by two investigators in a masked fashion (JSS and TPK).

This study was designed as cross-sectional, in which eyes with focal NFL defects were compared to control eyes over a relatively short period of time.

We calculated a mean of IOP measurements during all visits included into this study. The clinical data (e.g., IOP measurements) during one or more visits per patient were included into the study if recorded the same day as the OCT examination.

Criteria used to identify normal subjects were no history of glaucoma, retinal pathology, or intraocular surgery; best-corrected visual acuity of 20/40 or better; normal Humphrey 24–2 visual field; IOPs of 21 mmHg or lower; and no obvious pathology of the optic nerve or NFL by stereoscopic slit-lamp biomicroscopy.

The entry criteria used to identify glaucoma suspects were no history of intraocular surgery or retinal pathology, normal Humphrey 24–2 visual field testing, IOPs between 24 and 30 mmHg, and/or abnormal or asymmetric cupping of the optic nerve heads.

Criteria used to identify study subjects were focal defects of the NFL detected by slit-lamp biomicroscopic examination that were adjacent to the optic disc border during at least one visit. Although the criteria to identify study subjects were not based on the results of Humphrey visual field testing, most focal NFL defects corresponded to localized deep Humphrey 24–2 visual field defects with elevated corrected pattern standard deviation values. Early glaucoma was defined as patients who did not have complete loss of the neuroretinal rim in any quadrant and had visual field loss only on one side of the horizontal meridian by Humphrey 24–2 visual field testing. Advanced glaucoma was defined as a complete loss of the neuroretinal rim or visual field loss above and below the horizontal meridian.[22]

According to our previous findings of approximately 10-μm thinning of the NFL for each 10 years of age, we allowed a difference of ±5 years between the study subject and control patients (normal and glaucoma-suspect patients).[22] We included any patient meeting the criteria for our study or control group during the above-mentioned period.

Optical Coherence Tomography Technology

Optical coherence tomography is a new optical technique for high-resolution measurements and cross-sectional imaging of the retina and the NFL in particular. Measurements are performed using a fiber-optically integrated Michelson interferometer with a short coherence length superlumnescent diode source. One arm of the interferometer is a modular probe that directs light onto the subject and collects the retroflected signal. A second arm of the interferometer includes a translating retroflecting mirror. Interference is observed only when the optical path lengths of the two arms are matched to within the coherence length of the light source (typically approximately 10–20 μm). Translating the reference mirror and demodulating the interference signal at the detector produce a 1-diopter (D) depth reflectivity or low coherence interferometry.[23–30] Unlike optic nerve head analyzers, Heidelberg Retinal Tomographs, and other new optical devices, OCT requires no reference plane. Optical coherence tomography provides an absolute measurement of retinal substructure from which the NFL thickness is calculated. Near-infrared illumination (840 nm) is used to minimize patient discomfort. The OCT system was integrated into a conventional slit-lamp biomicroscope using fiber optics: the slit-lamp biomicroscope, a +78-D condensing lens mounted on the slit-lamp in front of the eye, and an attached infrared-sensitive video camera provided a view of the scanning beam on the fundus. Axial reflectance profiles (A-scans) are measured versus depth. Tomographic images are constructed from a series of A scans while scanning across the retina. We have used a computer algorithm to quantitate NFL and retinal thickness. The data are displayed as a two-dimensional false-color image in real time on a computer monitor.[22]

The limit for safe ocular exposure to the low coherence light used in OCT is based on and documented by the American National Standards Institute. Optical coherence tomography imposes no known risk to the participating subject. The scan rate used for this study was 100 lateral pixel retinal tomograms with a depth of 3 mm taken in 2.4 seconds. The axial resolution was 14 μm in air and predicted a higher resolution value in vivo because of the differences in refractive indices. In structures with greater differences in reflectivity (e.g., vitreoretinal surface), we expected higher resolution values than in structures with similar reflectivity (e.g., between neurosensory layers of the retina). The transverse resolution was a function of size of the optical beam waist and the distance between pixel elements. The circular tomogram consisted of 100 A-scans obtained across a tissue area of 110 μm. For better readability, the images are displayed doubly expanded in the longitudinal plane.

Optical Coherence Tomography Technique

Each subject underwent circular scans around the center of the optic disc using a circle size of 3.4 mm, which provided measurements that allowed analysis of focal defects of the NFL. The circle size of 3.4 mm was selected for this study because it allowed measurements of the NFL in a thicker area than the 4.5-mm-diameter circle used previously, provided better reproducibility than the 2.9-mm diameter, and was unlikely to impinge on the ONH, even in eyes with large discs.[23]

Because the operator was provided with a video camera view of the scanning probe beam on the fundus and a computer monitor showing the OCT image acquired in real time, he was able to center the circular scan on the ONH while the subject fixated with the eye being studied (internal fixation technique). The internal fixation technique produced better reproducibility than the external fixation technique, in which the subject fixated with the other eye.[23] Fine positioning of the circular scan around the center of the optic disc was accomplished by keyboard control of the scan length, vertical and horizontal orientation, and position relative to the patient's fixation point. A computer-controlled, flashing fixation light provided in the eye being scanned permitted the location of repeat images to be consistent between follow-up visits. The offset in the vertical and horizontal planes of each scan relative to the computer-controlled fixation light was automatically recorded with each image so that the position of each scan on the fundus was accurately determined. The centering technique depended on the examiner's ability to perform fine positioning of the circular scan. Although the reproducibility of NFL thickness measurements of normal and glaucomatous eyes by OCT during several visits has been studied, the patient's position in the sagittal plane may influence the reproducibility of centering of OCT scans around optic discs.[23] The NFL thickness measurements of normal and glaucomatous eyes using OCT have proved to provide adequate reproducibility: in a series of three circular scans taken on five separate occasions using the internal fixation technique, OCT NFL thickness reproducibility, as measured by intraclass correlation coefficient, was found to be 0.56 in normal eyes and 0.52 in glaucomatous eyes, when placing a 3.4-mm-circle diameter around the center of the optic nerve.[23]

An OCT scan consisted of 100 OCT points, which were taken within 2.5 seconds. These 100 OCT points were analyzed to be able to detect such microstructural changes as focal defects. The OCT points 0 to 24 were defined as the thickness measurements done in the superotemporal quadrant, 25 to 49 in the superonasal quadrant, 50 to 74 in the inferonasal quadrant, and 75 to 99 in the inferotemporal quadrant in both right and left eyes (Fig 1).

Image Processing and Analysis

We used an image processing algorithm to remove eye motion artifacts and to quantify retinal and NFL thickness automatically after data collection. The algorithm determined the retinal thickness according to a characteristic reflection pattern using an edge detection technique: the

anterior border of the retina represented the first reflection in the vitreoretinal interface, and the anterior border of the choriocapillaris/retinal pigment epithelium corresponded to a highly reflective layer that ends at the scleral rim of the optic nerve head. The NFL was identified as a highly reflective layer at the vitreoretinal surface. Its posterior border was located for each longitudinal scan by searching from the photoreceptor layer anteriorly up to a certain threshold. This threshold was determined as a specific portion of highest reflectivity in each longitudinal scan. The thickness of the NFL corresponded to the thickness of the NFL measured histologically in previous studies.[22] The photoreceptor layer was assumed to represent the minimum reflective layer located in between the anterior and posterior borders of the retina. Shadowing, caused by blood vessels, was corrected through linear interpolation. The images were displayed in false-color, in which bright colors (red to white) corresponded to regions of high relative optical reflectivity or backscattering and dim colors (blue to black) represented areas of minimal or no relative reflectivity. The NFL and retinal pigment epithelium boundaries were automatically highlighted with a blue line, and the superficial surface of the retina was denoted with a white line. The thickness measurements were reported for each longitudinal scan. Detailed information is included in the Appendix section.

Computational and Statistical Methods for Optical Coherence Tomography

For each OCT scan, the first quartile (Q1, the 25th percentile value), third quartile (Q3, the 75th percentile value), and median NFL thickness values (over the 100 OCT points) were determined. For each OCT scan among the control eyes, the NFL thickness curves were standardized as follows: (NFL - median)*2/(Q3–Q1).

By standardizing, we eliminated much of the interperson variation in the level and shape of the NFL curves. If we are indeed measuring the NFL thickness correctly, a focal NFL defect should correspond to an aberration in the shape of the curve, not necessarily in its value. A young person with a focal NFL defect may have high values at almost all OCT points and low values at just a few OCT points corresponding to a focal NFL defect. Methods that consider the magnitude of the NFL measurements at the OCT points might well miss such a person. In contrast, an elderly control person may have relatively low values at all the OCT points but in the normal pattern. Methods that consider the magnitude of the measurements at the OCT points might falsely consider such a person to have a defect. Nonetheless, extremely low values may be indicative of a defect as well, so we also incorporated the measured values into our computations.

A regression was then done on the standardized values, regressing against the first eight sine and cosine terms of a potential Fourier expansion (used because the NFL thickness as a function of OCT point is a function on a circle, and Fourier's theorem says that such functions can be written as infinite series of the trigonometric functions sines and cosines). The first eight sines and cosines were chosen, because after that, the coefficients became too small to have much effect. Residuals (i.e., differences between the measured value and the value predicted by the regression model at each OCT point) from the overall regression curve were obtained. For each OCT point, the mean residual - 2.33 * (standard deviation of the residuals) among all scans of control subjects was determined. This estimates the first percentile of the residuals at each OCT point. In addition, the mean NFL thickness - 2.33 * (standard deviation of NFL thickness) was determined for each OCT point among the control subjects. This estimates the first percentile of the NFL values at each OCT point.

The case subjects' eyes were handled similarly. Each scan was standardized using its median and Q1 and Q3. Residuals (in this case, the difference between the measured value and the value predicted by the regression model for the control eyes at the same OCT point) were determined. If the residual for an OCT point was below the estimated first percentile of the residuals of the control eyes at that OCT point, the OCT point was considered abnormal.

Further, if the NFL thickness at an OCT point was less than the estimated first percentile of the NFL thickness of the control eyes at that OCT point, the OCT point was considered abnormal. An eye was considered abnormal if it had three "sequential" (i.e., skipping no more than one OCT point at a time) abnormal OCT points. Estimates of sensitivity and specificity of OCT were done by Poisson regression. All computations were performed using SAS commercial statistical software packages (SAS Institute Inc., Cary, NC).[31,32]

Results

In the study group, we followed 25 eyes of 19 patients. The majority of study patients were women (18 women, 1 man). Focal defects were diagnosed bilaterally in six women. In one man, we detected a unilateral focal defect during NFL examination with slit-lamp biomicroscopy. In the control group, we followed 12 eyes of 6 women and 16 eyes of 8 men. The mean age was 61 ± 11 years among the study subjects and 58 ± 11 years among the control subjects.

The sensitivity of our criteria was 65% in the study eyes. The specificity of our criteria among control eyes was 81%. Most focal defects detected in the study eyes during OCT examination were in the same quadrant as observed during clinical NFL examination. Comparison of overall standardized NFL thickness values between the study and control eyes did not yield significant differences, because each study eye's focal NFL defect was in a unique location (refer to section on computational and statistical methods). However, when the subgroup of study eyes with inferotemporal focal NFL defects (the largest group among our study eyes) was considered, the location of the focal NFL defects was clearly reflected in the NFL thickness measurements (Figs 2, 3).

Examples

General—Because of the idiosyncratic nature of glaucomatous NFL defects, the diagnostic value of OCT may be more clearly illustrated by individual results than by averaged data. Figures 4 through 8 show photographic, visual field, and OCT results from a representative control eye and four glaucomatous eyes. Circular OCT scans using a scan diameter of 3.4 mm around the center of the optic disc are shown in part D of Figures 4 through 8. The NFL and retinal pigment epithelium boundaries were automatically highlighted with a blue line and the superficial surface of the retina with a white line (part D, Figs 4–8). Although parts D and E of Figures 4 through 8 represent the same data, it may be difficult to see the correspondence, because it is not easy to determine which OCT points were averaged in each region or to average these visually perceived OCT points.

Control Eye (Control 18)—A 62-year-old white man receiving no ocular medications presented with a normal eye examination. His left eye had a visual acuity of 20/20, and we measured an IOP of 10 mmHg. He showed a healthy optic disc and no NFL defects during dilated slit-lamp examination in his left eye and full Humphrey visual field. The NFL was thickest in the superior and inferior quadrants, which correlates with the typical "double hump" pattern described by Caprioli et al[33] (Fig 4) and which appears as a bifusiform, or even quadrifusiform, pattern on circular OCT scans.

Glaucomatous Eyes

Case 17 A 36-year-old black woman with advanced childhood glaucoma was status postlaser trabeculoplasty. She was taking timolol 0.5% (Timoptic; Merck & Co., Inc., West Point, PA), dorzolamide 2% (Trusopt; Merck & Co., Inc., West Point, PA), dipivefrin 0.1% (Propine; Allergan, Inc., Irvine, CA), pilocarpine (Ocusert 40; Alza Pharmaceuticals, Palo Alto, CA), and apraclonidine 0.5% (Iopidine; Alcon, Fort Worth, TX). She had a visual acuity of 20/20

in her right eye and presented with an IOP of 22 mmHg. The dilated fundus examination showed a focal NFL defect inferotemporally and marked cupping of the optic disc. A superior paracentral scotoma was seen on the Humphrey visual field. The OCT examination showed significant thinning of the NFL, especially in the inferotemporal region (Fig 5).

Case 15 A 62-year-old white woman presented with advanced pseudoexfoliation glaucoma in her right eye. She was status post-laser peripheral iridectomy and was taking levobunolol 0.5% (Betagan; Allergan, Inc., Irvine, CA), pilocarpine 2% (Pilocar; CibaVision Ophthalmic, Duluth, GA), and dorzolamide 2% in her right eye. Her visual acuity was 20/20, and the IOP measured was 24 mmHg in the right eye. The dilated fundus examination showed thinning of the NFL inferotemporally and a corresponding attenuation of the neuroretinal rim. A superior paracentral scotoma in the visual field examination of her right eye corresponded well with the fundus examination (Fig 6).

Case 11 A 71-year-old woman with normal-tension glaucoma had undergone laser trabeculoplasty in her left eye. She was taking timolol 0.5% twice daily. She had a visual acuity of 20/25 and an IOP of 13 mmHg. Her optic disc was moderately cupped with an attenuated neuroretinal rim temporally. The NFL examination showed a focal defect superotemporally that correlated with an inferior arcuate scotoma on the Humphrey visual field in her left eye. The OCT showed a focal area of NFL thinning (Fig 7).

Case 22 A 59-year-old woman receiving no ocular medications presented with normal-tension glaucoma. Her left eye had a visual acuity of 20/60, and we measured an IOP of 17 mmHg. Her optic disc was moderately cupped with an attenuated neuroretinal rim temporally. The NFL examination showed a focal defect inferotemporally. A paracentral scotoma was found on the Humphrey visual field in her left eye. The OCT failed to show a focal area of NFL thinning (Fig 8).

Discussion

Several techniques for clinical NFL evaluation have been described. Ophthalmoscopic examination using red-free light and NFL photography have been used for many years, but these techniques are limited to eyes with clear media and to good cooperation of the patient and are difficult to perform and interpret. The slit-lamp biomicroscopic NFL examination and NFL photography evaluation are subjective and depend on the experience of the examiner (and also the photographer, as in the case of NFL photography).

Other technologies, such as scanning laser polarimetry, have been developed to measure the thickness of the NFL. This device is based on changes in polarization of light and retardation, which is related to the NFL thickness. Unfortunately, the NFL is not the only birefringent structure in the eye, and it remains unclear what the effects of corneal and lenticular birefringence and aging are on polarimetric measurements. Polarimetric measurements can be influenced by peripapillary atrophy or chorioretinal scars, which may occur in healthy eyes or eyes with disease other than glaucoma.[34]

Optical coherence tomography enables cross-sectional visualization and direct measurement of NFL thickness. Low coherence light is applied through a noncontact, non-invasive instrument and depicts the retinal microstructure with a resolution of 10 μm. We found good correlation of NFL measurements by OCT to histopathologic analysis (Huang LN, Schuman JS, Kloizman TP, et al. Poster presentation at the Association for Research in Vision and Ophthalmology Annual Meeting, 1997; and Schuman JS, Pedut–Kloizman T, Pieroth L, et al. Oral presentation at the Association for Research in Vision and Ophthalmology Annual

Meeting, 1996). The reproducibility of OCT measurements compares well with other currently available ophthalmic instrumentation designed for optic nerve and NFL analysis.[23,35–38]

In cross-sectional studies, focal defects are found in approximately 20% of glaucomatous eyes examined.[15] Quigley et al[2] divided the types of NFL defects of patients who developed a visual field defect within a period of 5 years into upper and lower NFL zones. He found bundle defects in 5% superiorly and 3% inferiorly.

The gender distribution in our study did not correlate with that of previously described reports of bundle defects of the NFL, as the majority of our study patients were female. This distribution would not be expected to influence NFL measurements, as reported previously.[22] It may indeed be that focal defects actually occur more frequently in women than in men; however, the number of study subjects in our study was not high enough to address this question. It is likely that this gender imbalance merely reflected the nature of our patient pool.

There are discrepancies in the literature about the pathogenesis of focal and diffuse defects of the NFL. Samuelson and Spaeth[39] found a significantly lower maximal pretreatment IOP among patients with focal visual field defects than among those with diffuse visual field loss. Most of the patients analyzed also had focal NFL defects. Vascular, structural, and mechanical factors may increase laminar susceptibility, independent of IOP.

We chose to differentiate focal NFL defects from focal visual field defects because visual field changes in the earlier stages of glaucoma are difficult to track and can show a heterogenous pattern.[1–4,13,40] Based on findings in the studies cited above, we conclude that evaluation of the NFL may be superior to visual field testing in the earliest stages of glaucoma, because of its high sensitivity.

Future studies will investigate in more detail which longitudinal changes in NFL thickness occur in patients with glaucoma. Furthermore, we expect additional refinements in our diagnostic criteria as more normative OCT data become available.

Localized NFL defects seem to occur in the early stages of glaucoma and are sometimes associated with optic disc hemorrhages. The stages of glaucoma in our study correlated with previously described focal defects of the NFL.[14,16,17,21,41] Most case subjects in our study had early glaucoma. In this study, it is not possible to determine whether the focal defects preceded the development of diffuse defects.

The location of the focal NFL defects in this study also correlated with previously described focal defects. The focal NFL defects were located in the inferotemporal and superotemporal regions of the NFL. Jonas et al[42,43] similarly found that focal NFL defects occur significantly more often in the inferior fundus region, followed by the superior areas and the temporal region.

We found a specificity of 81% and a sensitivity of 65% of detecting focal defects solely through statistical analysis of OCT measurements (i.e., without clinical interpretation of the tomographic OCT scan). Sensitivity may improve when more normative data are available.

Optical coherence tomography permits us to detect focal defects independent of the visibility of the NFL. Thus, the chances of detecting these defects in areas of physiologic decreased visibility are higher using OCT than compared to conventional clinical methods.[44]

We found that focal defects are often demarcated by blood vessels (Figs 5, 7, and 8); it is possible that blood vessels provide structural support for the NFL from the periphery toward the ONH.

Optical coherence tomography is an objective, reproducible, and sensitive tool to track localized defects of the NFL and may provide early detection of glaucomatous damage.[18, 45] Although clinical NFL examination has been recommended as a most sensitive indicator of glaucoma,[3,4] clinical examination is difficult and subjective, and NFL photography requires high technical skill. It is critical that accurate NFL assessment be performed by all clinicians; OCT not only facilitates NFL evaluation, but it permits quantitative, objective, and reproducible tissue measurements.

Acknowledgements

Supported by National Eye Institute, Rockville, Maryland, NIH 1-R29-EY11006-01, NIH 9-RO1-EY11289, MFEL N00014-94-1-0717. Also supported by the Fight for Sight research division of Prevent Blindness America, Schaumburg, SF96031 (LP).

References

1. Quigley HA, Addicks EM, Green WR. Optic nerve damage in human glaucoma. III. Quantitative correlation of nerve fiber loss and visual field defect in glaucoma, ischemic neuropathy, papilledema, and toxic neuropathy. Arch Ophthalmol 1982;100:135–46. [PubMed: 7055464]
2. Quigley HA, Katz J, Derick RJ, et al. An evaluation of optic disc and nerve fiber layer examinations in monitoring progression of early glaucoma damage. Ophthalmology 1992;99:19–28. [PubMed: 1741133]
3. Sommer A, Miller NR, Pollack I, et al. The nerve fiber layer in the diagnosis of glaucoma. Arch Ophthalmol 1977;95:2149–56. [PubMed: 588106]
4. Sommer A, Katz J, Quigley HA, et al. Clinically detectable nerve fiber atrophy precedes the onset of glaucomatous field loss. Arch Ophthalmol 1991;109:77–83. [PubMed: 1987954]
5. Airaksinen PJ, Drance SM, Douglas GR, et al. Visual field and retinal nerve fiber layer comparisons in glaucoma. Arch Ophthalmol 1985;103:205–7. [PubMed: 3977691]
6. Drance SM, Airaksinen PJ, Price M, et al. The correlation of functional and structural measurements in glaucoma patients and normal subjects. Am J Ophthalmol 1986;102:612–6. [PubMed: 3777081]
7. Tuulonen A, Lehtola J, Airaksinen PJ. Nerve fiber layer defects with normal visual fields. Do normal optic disc and normal visual field indicate absence of glaucomatous abnormality? Ophthalmology 1993;100:587–98. [PubMed: 8493001]
8. Airaksinen PJ, Alanko HI. Effect of retinal nerve fibre loss on the optic nerve head configuration in early glaucoma. Graefes Arch Clin Exp Ophthalmol 1983;220:193–6. [PubMed: 6884783]
9. Minckler DS. The organization of nerve fiber bundles in the primate optic nerve head. Arch Ophthalmol 1980;98:1630–6. [PubMed: 6158937]
10. Quigley, HA. Diagnosing early glaucoma with nerve fiber layer examination. New York, Tokyo: Igaku–Shoin; 1996.
11. Airaksinen PJ, Drance SM. Neuroretinal rim area and retinal nerve fiber layer in glaucoma. Arch Ophthalmol 1985;103:203–4. [PubMed: 3977690]
12. Jonas JB, Schiro D. Localized retinal nerve fiber layer defects in nonglaucomatous optic nerve atrophy. Graefes Arch Clin Exp Ophthalmol 1994;232:759–60. [PubMed: 7890191]
13. Iwata K, Nanba K, Abe H. Die beginnende Fundusveränderung infolge rezidivierender kleiner Krisen beim Posner-Schlossman- Syndrom — ein Modell für das Glaucoma simplex. Klin Monatsbl Augenheilkd 1982;180:20–6. [PubMed: 7077989]
14. Jonas JB, Dichtl A. Evaluation of the retinal nerve fiber layer. Surv Ophthalmol 1996;40:369–78. [PubMed: 8779083]
15. Jonas JB, Schiro D, Naumann GOH. Retinale Nervenfaserschicht in Normal- und Glaukomaugen. Ophthalmologe 1993;90:603–12. [PubMed: 8124022]
16. Airaksinen PJ, Tuulonen A. Early glaucoma changes in patients with and without an optic disc haemorrhage. Acta Ophthalmol 1984;62:197–202. [PubMed: 6720285]
17. Airaksinen PJ, Drance SM, Douglas GR, et al. Diffuse and localized nerve fiber layer loss in glaucoma. Am J Ophthalmol 1984;98:566–71. [PubMed: 6496612]

18. Schuman, JS. Imaging of the optic nerve head and nerve fiber layer in glaucoma. In: Epstein, DL.; Allingham, RR.; Schuman, JS., editors. Chandler and Grant's Glaucoma. 4. chap. 9. Baltimore: Williams & Wilkins; 1996.
19. Mattox, C. Clinical examination of the nerve fiber layer. In: Schuman, JS., editor. Imaging in Glaucoma. chap. 5. Thorofare, NJ: Slack Inc; 1996.
20. Quigley HA, Coleman AL, Dorman–Pease ME. Larger optic nerve heads have more nerve fibers in normal monkey eyes. Arch Ophthalmol 1991;109:1441–3. [PubMed: 1929937]
21. Tuulonen A, Airaksinen PJ. Initial glaucomatous optic disk and retinal nerve fiber layer abnormalities and their progression. Am J Ophthalmol 1991;111:485–90. [PubMed: 2012151]
22. Schuman JS, Hee MR, Puliafito CA, et al. Quantification of nerve fiber layer thickness in normal and glaucomatous eyes using optical coherence tomography: a pilot study. Arch Ophthalmol 1995;113:586–96. [PubMed: 7748128]
23. Schuman JS, Pedut–Kloizman T, Hertzmark E, et al. Reproducibility of nerve fiber layer thickness measurements using optical coherence tomography. Ophthalmology 1996;103:1889–98. [PubMed: 8942887]
24. Swanson EA, Izatt JA, Hee MR, et al. In vivo retinal imaging by optical coherence tomography. Opt Lett 1993;18:1864.
25. Huang D, Swanson EA, Lin CP, et al. Optical coherence tomography. Science 1991;254:1178–81. [PubMed: 1957169]
26. Izatt, JA.; Hee, MR.; Huang, D., et al. Ophthalmic diagnostics using optical coherence tomography. In: Parel, J-M.; Ren, Q., editors. Proceedings of Ophthalmic Technologies III; 16–18 January 1992; Los Angeles, California. Bellingham, Wash, USA: SPIE; 1993. p. 136-44.(Proc. of SPIE — The International Society for Optical Engineering; v. 1877) (Progress in Biomedical Optics)
27. Hee MR, Izatt JA, Swanson EA, et al. Optical coherence tomography of the human retina. Arch Ophthalmol 1995;113:325–32. [PubMed: 7887846]
28. Izatt JA, Hee MR, Swanson EA, et al. Micrometer-scale resolution imaging of the anterior eye in vivo with optical coherence tomography. Arch Ophthalmol 1994;112:1584–9. [PubMed: 7993214]
29. Puliafito CA, Hee MR, Lin CP, et al. Imaging of macular diseases with optical coherence tomography. Ophthalmology 1995;102:217–29. [PubMed: 7862410]
30. Hee MR, Puliafito CA, Wong C, et al. Optical coherence tomography of macular holes. Ophthalmology 1995;102:748–56. [PubMed: 7777274]
31. Littel, RC.; Milliken, GA.; Stroup, WW.; Wolfinger, RD. SAS Institute System for Mixed Models. Cary, NC: SAS Institute; 1996.
32. Morrison, DF. Multivariate Statistical Methods. New York, NY: McGraw–Hill; 1976. p. 141-53.
33. Caprioli J, Ortiz–Colberg R, Miller JM, Tressler C. Measurements of peripapillary nerve fiber layer contour in glaucoma. Am J Ophthalmol 1989;108:404–13. [PubMed: 2679110]
34. de Souza Lima, M.; Zangwill, L.; Weinreb, RN. Scanning laser polarimetry to assess the nerve fiber layer. In: Schuman, JS., editor. Imaging in Glaucoma. Thorofare, NJ: Slack; 1997. p. 83-92.
35. Dreher AW, Tso PC, Weinreb RN. Reproducibility of topographic measurements of the normal and glaucomatous optic nerve head with the laser tomographic scanner. Am J Ophthalmol 1991;111:221–9. [PubMed: 1992744]
36. Kruse FE, Burk ROW, Völcker HE, et al. Reproducibility of topographic measurements of the optic nerve head with laser tomographic scanning. Ophthalmology 1989;96:1320–4. [PubMed: 2780001]
37. Weinreb RN, Lusky M, Bartsch DU, Morsman D. Effect of repetitive imaging on topographic measurements of the optic nerve head. Arch Ophthalmol 1993;111:636–8. [PubMed: 8489444]
38. Weinreb RN, Shakiba S, Zangwill L. Scanning laser polarimetry to measure the nerve fiber layer of normal and glaucomatous eyes. Am J Ophthalmol 1995;119:627–36. [PubMed: 7733188]
39. Samuelson TW, Spaeth GL. Focal and diffuse visual field defects: their relationship to intraocular pressure. Ophthalmic Surg 1993;24:519–25. [PubMed: 8233314]
40. Quigley HA, Dunkelberger GR, Green WR. Retinal ganglion cell atrophy correlated with automated perimetry in human eyes with glaucoma. Am J Ophthalmol 1989;107:453–64. [PubMed: 2712129]

41. Iwata K, Kurosawa A, Sawaguchi S. Wedge-shaped retinal nerve fiber layer defects in experimental glaucoma preliminary report. Graefes Arch Clin Exp Ophthalmol 1985;223:184–9. [PubMed: 4054640]

42. Jonas JB, Schiro D. Localised wedge shaped defects of the retinal nerve fibre layer in glaucoma. Br J Ophthalmol 1994;78:285–90. [PubMed: 8199115]

43. Jonas JB, Fernández MC, Stürmer J. Pattern of glaucomatous neuroretinal rim loss. Ophthalmology 1993;100:63–8. [PubMed: 8433829]

44. Jonas JB, Nguyen NX, Naumann GOH. The retinal nerve fiber layer in normal eyes. Ophthalmology 1989;96:627–32. [PubMed: 2748120]

45. Quigley HA, Addicks EM. Quantitative studies of retinal nerve fiber layer defects. Arch Ophthalmol 1982;100:807–14. [PubMed: 7082210]

46. Hee, MR. PhD Thesis. Department of Electrical Engineering and Computer Science; Massachusetts Institute of Technology: Feb. 1997 Optical Coherence Tomography of the Eye.

Appendix

Image processing techniques were used to automatically extract measurements of retinal nerve fiber layer (NFL) thickness from each A-scan in the tomogram and are described in detail in reference 47. In brief, the computer algorithm consisted of the following steps: (1) logarithmic transformation; (2) A-scan registration; (3) smoothing; (4) identification of the vitreoretinal interface, retinal pigment epithelium, and photoreceptor layer; (5) threshold selection; (6) identification of the posterior boundary of the NFL; and (7) calculation of NFL thickness.

In step (1), the absolute value of optical reflectivity represented by each pixel in the image was transformed into a relative logarithmic (decibel) scale in which the standard deviation of the noise in the image corresponded to a level of 0 dB. Thus, the minimum detectable reflectivity was approximately 6 dB. All future calculations were performed using this logarithmic representation. In step (2), each A-scan comprising the tomogram was registered in the longitudinal direction to account for involuntary axial eye motion. In this step, the A-scans were individually shifted in the longitudinal direction to make the retinal contour appear flat. Registration was accomplished by cross-correlating each A-scan with its nearest neighbor to determine the offset (corresponding to the peak cross-correlation value) at which adjacent scans were maximally similar. In step (3), speckle noise in the image was reduced by two-dimensional linear convolution with an 11 × 11 element center weighted kernel that was approximately a low-pass filter with a cutoff frequency of 0.1 pi radians in both dimensions. The kernel was created by repeated self-convolution with the following 3 × 3 matrix: 1/16* [1 2 1; 2 4 2; 1 2 1]. In step (4), the boundaries of the neurosensory retina were identified by using an edge detection technique. Each A-scan was convolved with an 11-element column vector [-1 -1 -1 -1 -1 0 1 1 1 1 1] to identify sharp transitions that might indicate horizontal edges. The largest two peaks in each resulting column vector generally corresponded to (1) the high contrast in reflectivity between the nonreflective vitreous and the reflective NFL and (2) the contrast between the minimally reflective photoreceptive layer and the highly reflective retinal pigment epithelium and choriocapillaris. An error-correcting step was used to interpolate these two boundaries in situations in which an edge might be obscured. The anterior boundary of the NFL was assumed to lie at the vitreoretinal interface. The posterior boundary of the NFL was known to occur somewhere between the vitreoretinal interface and the location of the photoreceptor layer. The location of the photoreceptor layer was established for each A-scan as the position of minimum reflectivity within the posterior of the area between the vitreoretinal interface and the retinal pigment epithelium. In step (5), a threshold value was calculated for each A-scan separately to account for variations in optical alignment and media opacity across the image. The maximum values of reflectivity for each A-scan (after smoothing and logarithmic transformation) were compiled into a row vector, and a constant (15 dB) was subtracted from each row vector element to provide an initial value for the thresholds. The row

vector of thresholds was then smoothed to remove extreme values by circular convolution with a 21-element Blackman windowed finite-impulse response low-pass digital filter with a cutoff frequency of pi/10 radians. In step (6), the location of the posterior boundary of the NFL was determined using the threshold value calculated in step (5). Pixels in each smoothed A-scan were evaluated in anterior direction starting at the photoreceptor layer until a superthreshold reflectivity was encountered. The location of this first superthreshold pixel established the initial location of the posterior NFL boundary. Then, starting at the vitreoretinal interface, pixels were evaluated in a posterior direction until the first subthreshold pixel after a superthreshold pixel was located. If the pixels located by the two searches were adjacent to each other, then the posterior NFL boundary was confirmed. If the two pixels were separated, then one of these pixels was chosen as the location of the NFL boundary based on the average reflectivity of the intervening pixels. If the average reflectivity exceeded the threshold, then the deeper pixel was selected; otherwise, the shallower pixel was selected. Both an anterior search and a posterior search were performed to reduce potential variability due to spurious intraretinal reflections. For clinical review, all boundaries demarcated by the computer were shown overlayed on the optical coherence tomographic images. In step (7), retinal thickness was calculated from the number of pixels between the inner and outer retinal boundaries. A constant retinal refractive index of 1.36 was assumed to convert time-of-flight delay to intraretinal distance. This assumption was expected to induce a negligible error in the thickness measurements because the refractive index was expected to deviate no more than 5% from the estimated value. Consider that the difference in refractive index between the retina and water is only 2%. A 5% difference in index over the entire NFL thickness of approximately 100.5 μm would result in a 5.5-μm error in measurement, which is negligible compared to the longitudinal resolution of the instrument.

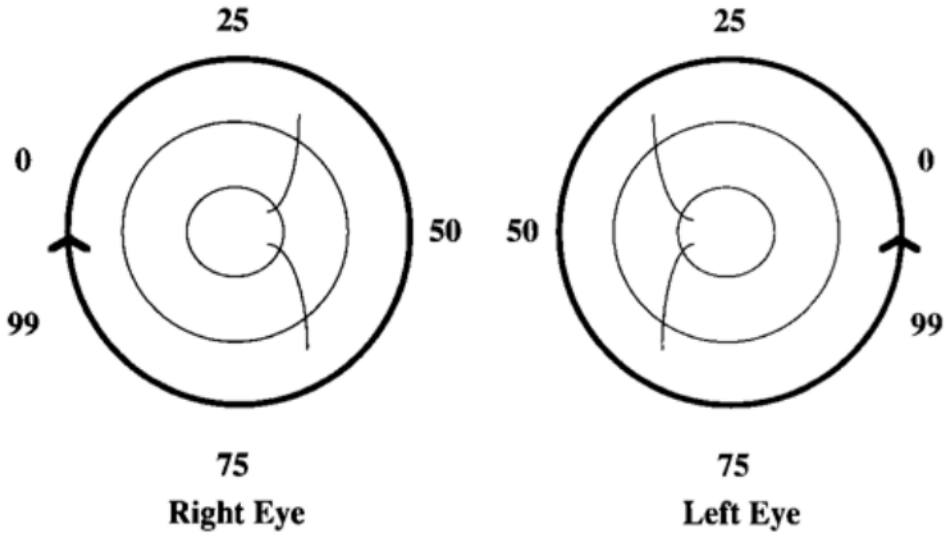

Figure 1.
Schematic diagram of the 100 optical coherence tomography points taken within 2.5 seconds.

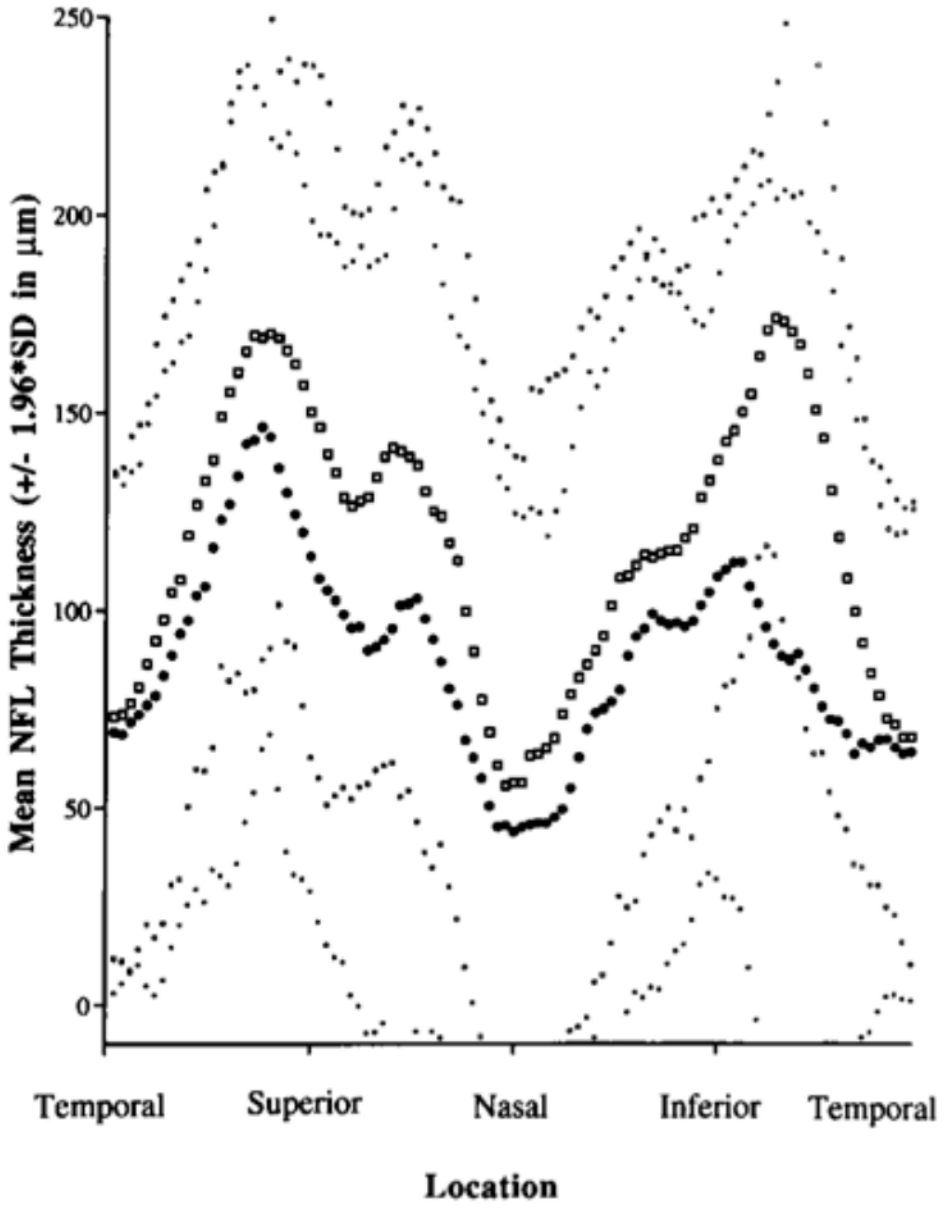

Figure 2.
Optical coherence tomography graph illustrating the mean peripapillary nerve fiber layer (NFL) thickness (±1.96*standard deviation) of all control eyes (open squares) compared to all eyes with inferotemporal NFL defects (filled circles). Note that the overall shapes of the two curves are similar. SD = standard deviation.

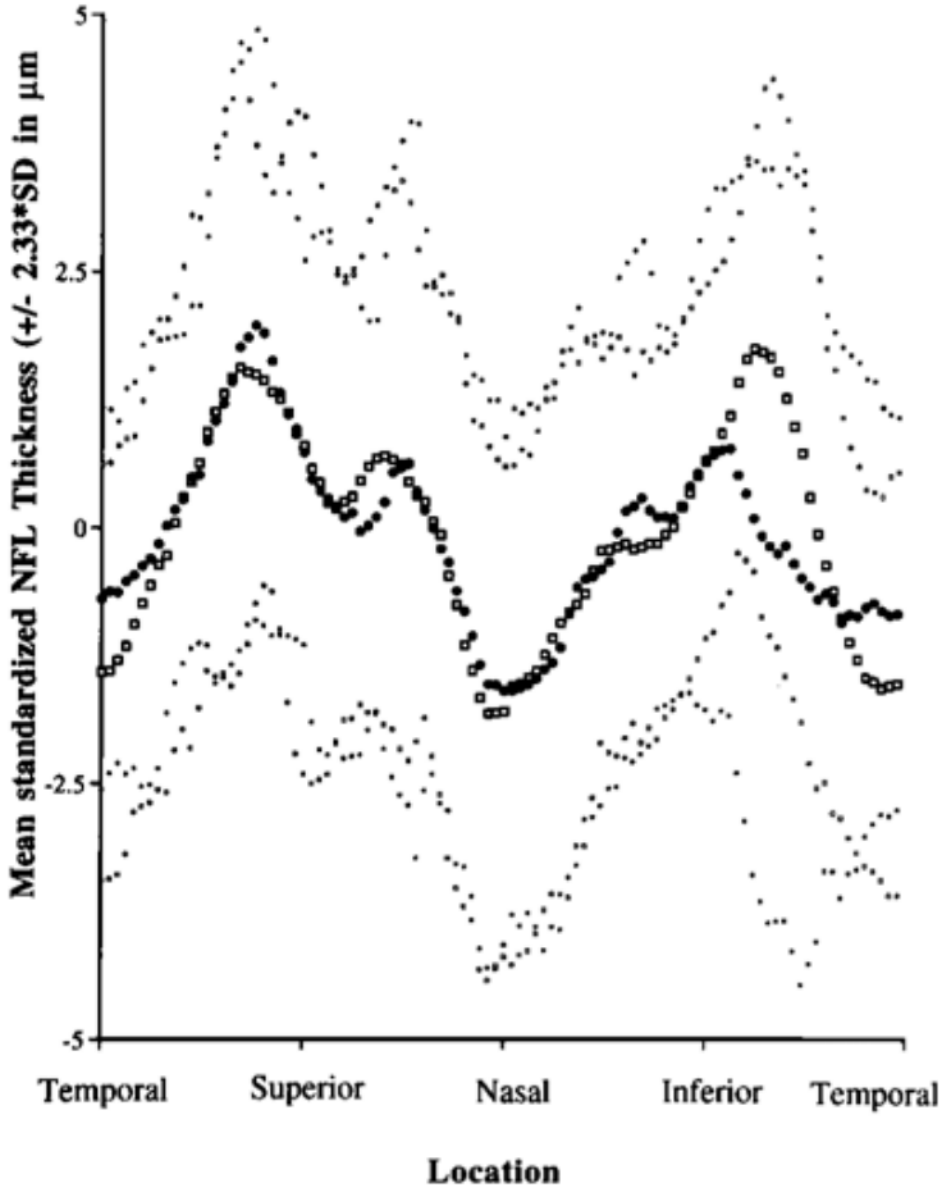

Figure 3.
Optical coherence tomography graph illustrating the mean standardized peripapillary nerve fiber layer (NFL) thickness (±2.33*standard deviation) of all control eyes (open squares) compared to all eyes with inferotemporal NFL defects (filled circles). Note that the mean standardized values at the optical coherence tomography points for the study eyes are almost the same as those for the control eyes, except for the inferotemporal region. SD = standard deviation.

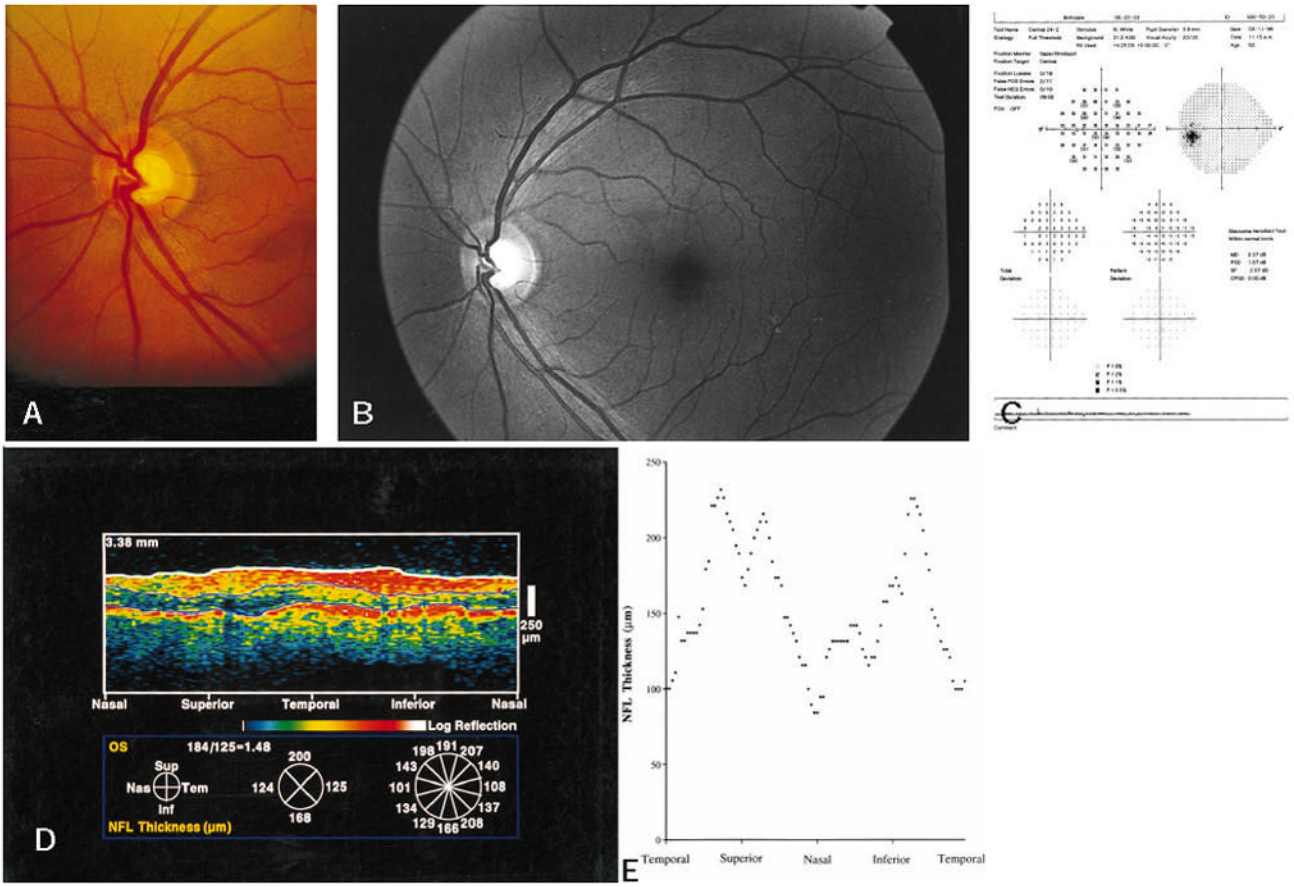

Figure 4. Control 18

A, stereoscopic optic nerve head photography of a control eye. **B,** red-free nerve fiber layer (NFL) photograph of the control eye. **C,** full Humphrey 24–2 visual field. **D,** circular optical coherence tomography (OCT) scan shows normal NFL thickness values in all four quadrants. **E,** OCT graph depicting 100 OCT points taken within 2.5 seconds. MD = mean deviation; CPSD = corrected pattern standard deviation.

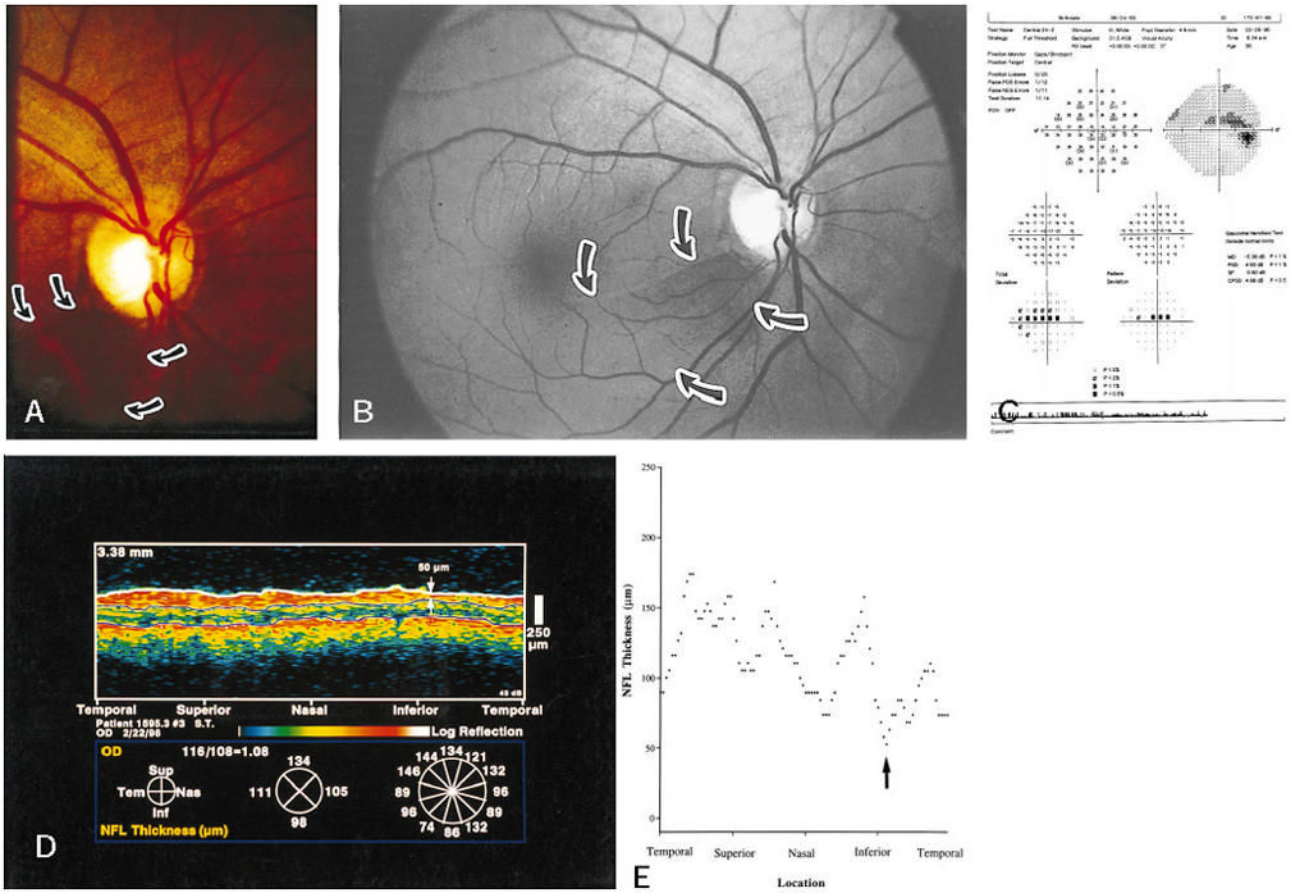

Figure 5. Case 17

A, stereoscopic optic nerve head photograph of the right eye with moderate cupping of the optic disc and a localized arcuate nerve fiber layer (NFL) defect inferotemporally. **B,** red-free NFL photograph shows the localized arcuate NFL defect inferotemporally (arrows). Note that a blood vessel demarcates the focal NFL defect inferiorly. **C,** Humphrey 24–2 visual field shows a superior cecocentral scotoma. **D,** circular optical coherence tomograph (OCT) shows significant thinning of the NFL, especially in the inferotemporal region. **E,** OCT graph shows focal thinning in the inferotemporal NFL.

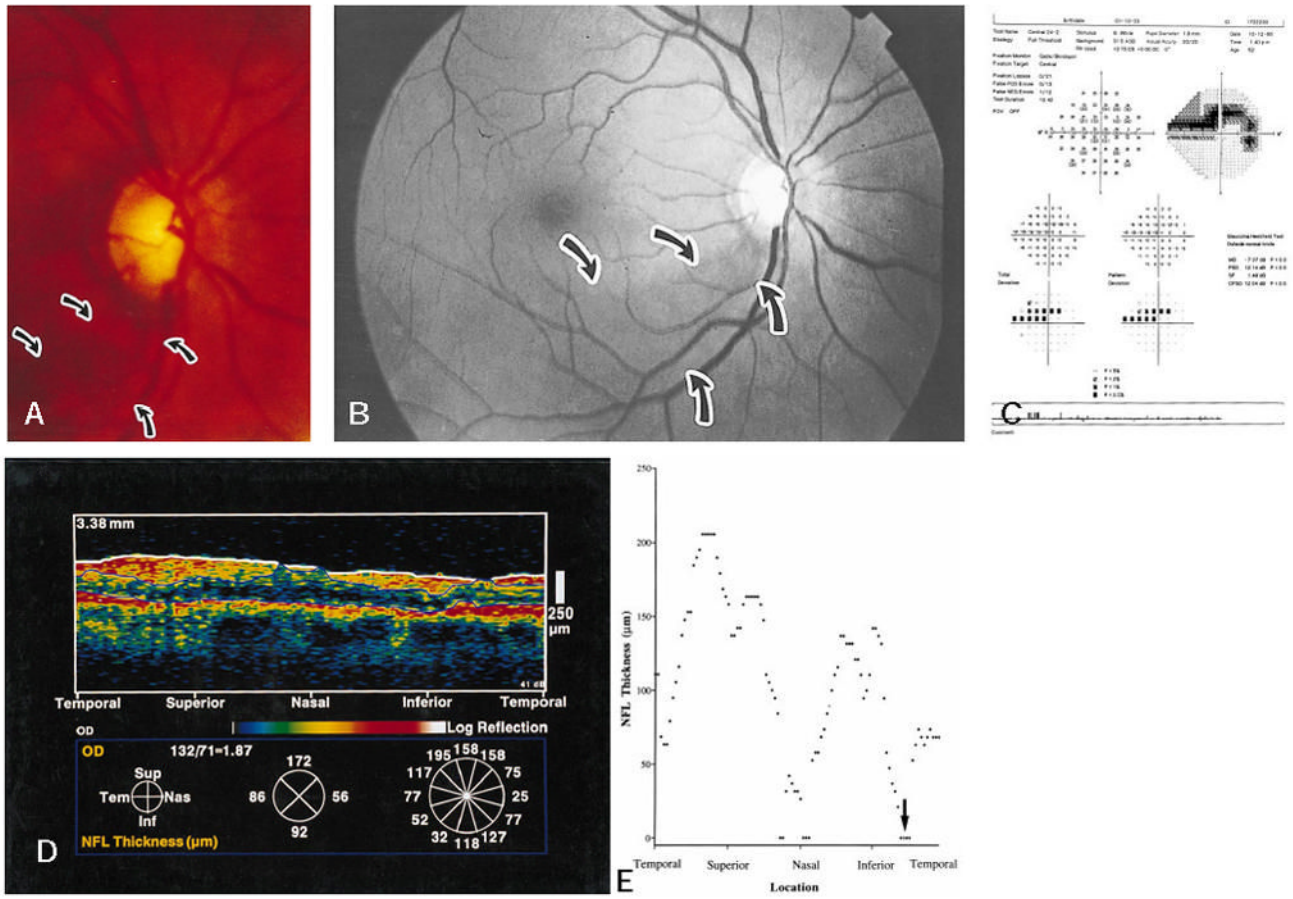

Figure 6. Case 15

A, stereoscopic optic nerve head photograph of the right eye in a subject with a localized arcuate nerve fiber layer (NFL) defect inferotemporally (arrows). **B,** red-free NFL photograph shows the localized arcuate NFL defect inferotemporally (arrows). **C,** Humphrey 24–2 visual field shows a superior paracentral defect corresponding with the inferotemporal defect. **D,** circular optical coherence tomograph (OCT) shows significant thinning of the NFL, especially in the inferotemporal region. **E,** OCT graph shows focal thinning in the inferotemporal NFL.

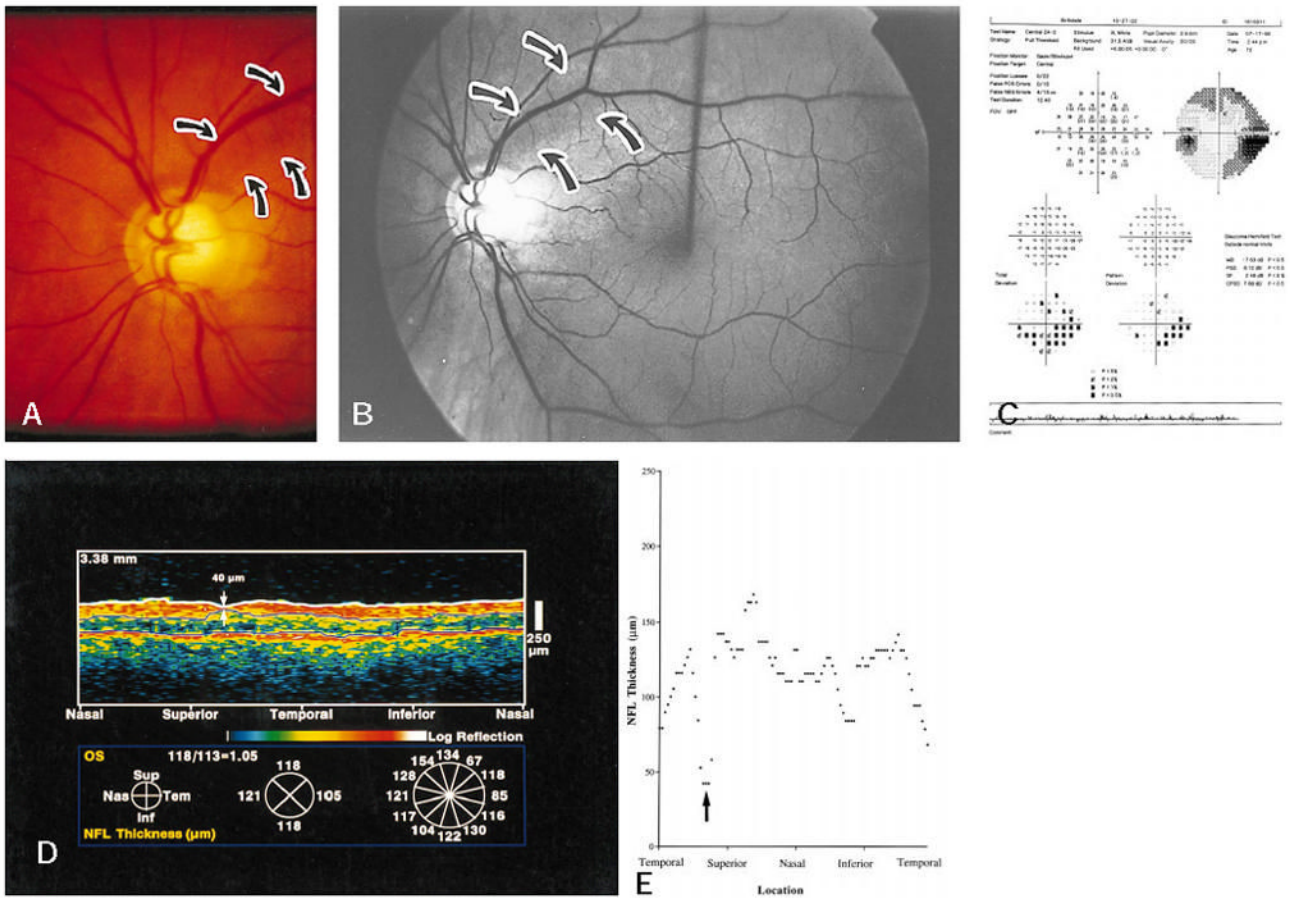

Figure 7. Case 11

A, stereoscopic optic nerve head photograph of the left eye in a subject with a localized arcuate nerve fiber layer (NFL) defect superotemporally (arrows). **B,** red-free NFL photograph shows the localized arcuate NFL defect superotemporally (arrows). Note that a blood vessel demarcates the focal NFL defect superiorly. **C,** Humphrey 24–2 visual field shows an inferior arcuate defect. **D,** circular optical coherence tomograph (OCT) shows focal thinning of the NFL (arrow). **E,** OCT graph shows thinning in the superotemporal NFL.

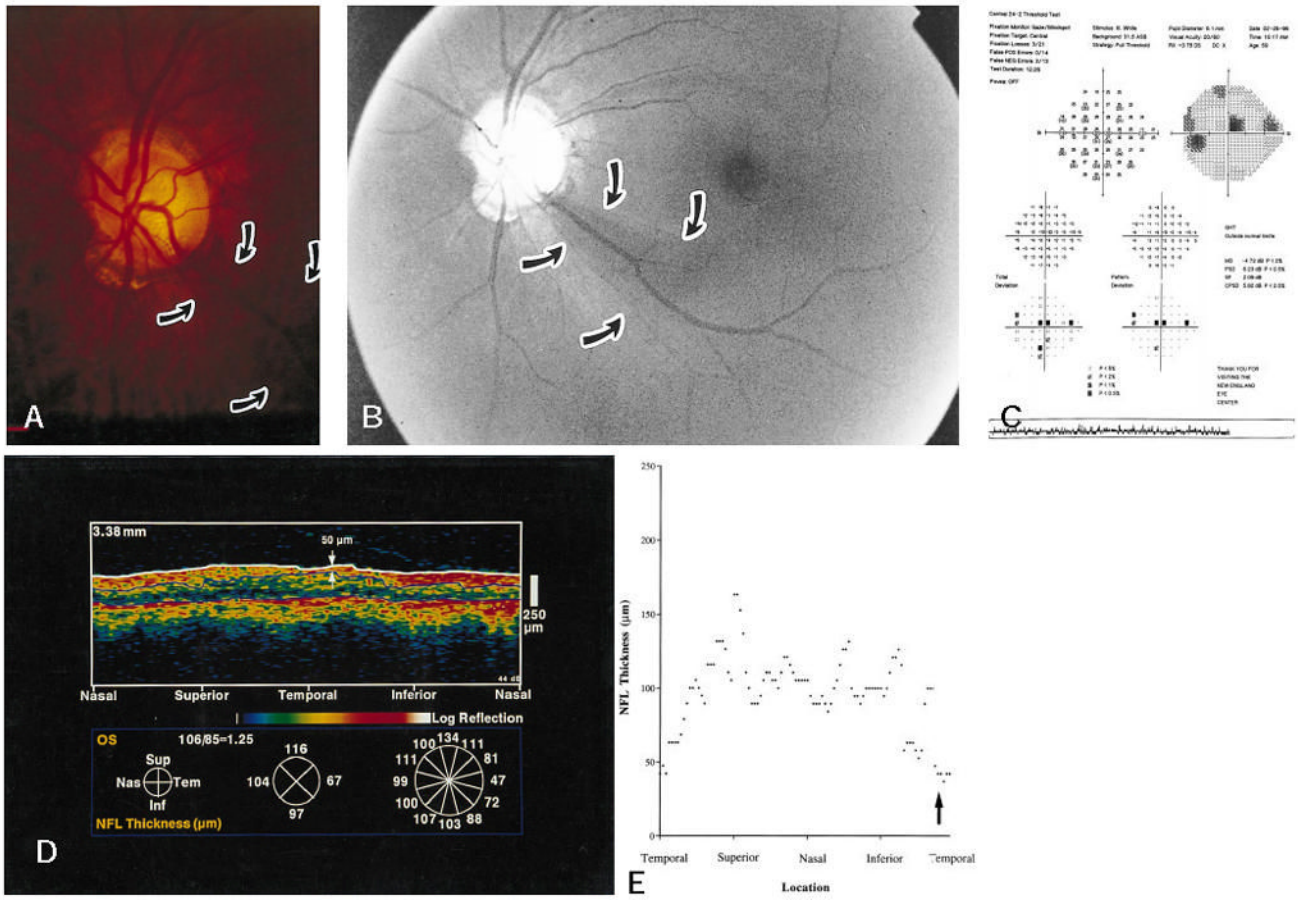

Figure 8. Case 22

A, stereoscopic optic nerve head photograph of the left eye in a subject with a localized arcuate nerve fiber layer (NFL) defect inferotemporally (arrows). **B,** red-free NFL photograph shows the localized arcuate NFL defect inferotemporally (arrows). Note that blood vessels demarcate the focal NFL defect superiorly and inferiorly. **C,** Humphrey 24–2 visual field shows a paracentral defect. **D,** circular optical coherence tomograph (OCT) fails to show focal thinning of the NFL inferotemporally (arrow). **E,** OCT graph fails to show excess thinning in the inferotemporal NFL.